



ISSN: 0067-2904

## A Gray Scale Image Compression Using Hierarchical DWT Decomposition and Mixing Quantization Techniques

Noor Sabah Mahdi\* , Ghadah Al-Khafaji

Department of Computers, College of Science, University of Baghdad, Baghdad, Iraq

Received: 20/3/2023

Accepted: 26/8/2023

Published: 30/10/2024

### Abstract

This paper describes a hybrid grayscale compression system based on the discrete wavelet transform (DWT) and a polynomial coding technique for mixing quantization schemes to increase the compression ratio while maintaining quality. The proposed compression system consists of three main steps: first, decomposing an image using a three-level DWT; second, applying the 2-D linear polynomial coding technique to the approximation sub-band; and third, dividing the detailed sub-bands of each level into the Most Significant Value (MSV) and Least Significant Value (LSV), where the former is compressed using iterative scalar uniform quantization and the latter by soft quantization thresholding. For testing the performance of the suggested compression system, five standard images of size 256×256 pixels were adopted. The suggested technique showed superior performance in terms of reconstructed (decoded) image quality and compression ratio (gain), where the compression ratio is between 21–27 with a PSNR value between 36–38 dB and the compression ratio of JPEG is between 7–20 with a PSNR value between 33–37 dB.

**Keywords:** Discrete wavelet transform, Image data compression, 2-D linear polynomial coding technique, Most and least significant values, Soft quantization thresholding technique.

### ضغط صورة بمقياس رمادي باستخدام تقنيات التحلل الهرمي المنفصل لتحويل الموجة والخلط

نور صباح مهدي\* ، غادة الخفاجي

قسم الحاسبات، كلية العلوم، جامعة بغداد، بغداد، العراق.

### الخلاصة

قدم هذا البحث نظام ضغط هجين للصور الرمادية حيث يعتمد على التحويل الموجي المنفصل (DWT) وتقنية الترميز متعدد الحدود لخلط مخططات التكميم لزيادة نسبة الضغط مع الحفاظ على الجودة. يتكون نظام الضغط المقترح من ثلاث خطوات رئيسية ، أولاً ، تفكيك الصورة بواسطة DWT ثلاثي المستويات ، متبوعاً بتطبيق تقنية التشفير الخطي متعدد الحدود ثنائي الأبعاد على النطاق الفرعي التقريبي ، ثم فصل النطاقات الفرعية التفصيلية لكل مستوى إلى القيمة الأكثر أهمية (MSV) والأقل أهمية (LSV) ، حيث يتم ضغط الأول بواسطة تكميم منتظم عددي متكرر ، بينما يتم ضغط الأخير بواسطة مخطط عتبة تكميم ناعم. أظهرت التقنية المقترحة أداءً فائقاً من حيث جودة الصورة المعاد بناؤها (فك الشفرة) ونسبة الضغط (المكتسبة).

\*Email: [nour.sabbah1201a@sc.uobaghdad.edu.iq](mailto:nour.sabbah1201a@sc.uobaghdad.edu.iq)

## 1. Introduction

Nowadays, more than 65% of people around the world communicate online using multimedia tools (i.e., images, audio, and video) via social multimedia applications (Viber, WhatsApp), which come with two essential issues of storage capacity and/or transmission bandwidth [1–3].

Image data compression is a vital optimum solution that cuts storage costs and/or speeds transmission of compressed data by efficiently utilizing image data redundancy in statistical and/or psychovisual bases, which implicitly ground into lossless or lossy techniques, respectively [4–7]. The former image compression techniques of lossless (identical) base, also referred to as information-preserving (error-free), had low compression performance due to exploiting the inter-pixel (spatial) and coding redundancies by utilizing techniques of lossless predictive coding and symbol encoders either of entropy base (i.e., Huffman coding, Arithmetic coding) or probability base (Lempel-Ziv algorithm) [1, 8–13]. While the latter image compression techniques have a lossy (approximation) base and high compression performance due to exploiting the psychovisual redundancy with/without the statistical former one, with techniques such as fractal, block truncation coding (BTC), absolute BTC, JPEG, and JP2 [14–16].

Polynomial coding based on Taylor approximation modeling is usually put into groups based on the degree of approximation and the shape of the blocks. This means that linear and nonlinear approximations can be used with both 2D and 1D block shapes [3, 10, 17–21]. In spite of a number of researchers utilizing the techniques to compress images (gray or color), the techniques still suffer from large residualities.

This paper is concerned with an investigation of hybrid lossy image compression techniques in grayscale using DWT decomposition of Haar base with different quantization schemes, either uniformly or non-uniformly, according to the separation data values of LSV and MSV. The paper is organized as follows: Section 2 reviews the related works; Section 3 discusses the methodology of the suggested system in detail; and the following sections are concerned with the experimental results and conclusion.

## 2. Related work

Polynomial coding is a modeling-based technique for prediction and differentiation. This section focuses on the main efforts to improve or enhance the traditional polynomial coding techniques, either linear or non-linear, for 2D or 1D shapes of grayscale image bases. Rasha [22], which mixed between linear and non-linear polynomial models for 2D block shapes using edges and homogeneity measures for grayscale images, where the compression ratio is between 8 and 13, with PSNR values exceeding 32 dB, Athraa [23], Shymaa [24], Rana [25], and Abdullah et al. [17] exploited the hierarchal scheme efficiently along the 2D-linear polynomial coding of DWT decomposition, interpolation, and even-odd schemes, respectively. In [23], the compression ratio for grayscale images is between 3 and 9, with PSNR values between 32 dB and 52 dB on average. In [24], the compression ratio for color images varies between 6 and 14, with the PSNR values being between 28 dB and 32 dB.

In [25], the compression ratio for grayscale images is between 9 and 11. In [17], the compression ratio for natural grayscale images is between 7 and 8, while for medical images it exceeds 10. Different quantization techniques, such as those used by Ghadah et al. [26] and Ghadah [27] for hard/soft thresholding techniques and by midtread for 2D linear polynomial coding, are used to effectively quantify residual images.

In [26], the compression ratio is between 5 and 12, with PSNR values between 28 dB and 30 dB for grayscale images. In [27], the compression ratio exceeds 11, with PSNR values of 36 or more for grayscale images. Ghadah and Loay [28] showed that 1D linear polynomial coding with a non-uniform quantization residual image was better. Samara et al. [29] made it even better by using C621 to code the residual image with the Minimize Matrix Size Algorithm (MMSA) of the binary search algorithm base.

Rasha et al. [30] compressed gray biometric iris images without losing quality by combining the discrete Fourier transform (DFT) of conjugate symmetry with traditional polynomial coding. In [28], the compression ratio for grayscale images is between 5 and 9, with PSNR values between 35 dB and 38 dB. In [29], the compression ratio for grayscale images is between 9 and 11, with PSNR values between 39 dB and 40 dB. In [30], the compression ratio for grayscale images is between 7 and 8. Zainab et al. [31] improved lossy color polynomial coding of the YUV color transformation model by using variable block sizes and a quadtree partitioning scheme of residuals encoded based on a mix of LZW and run-length coding techniques. The compression ratio was more than 15, and the PSNR values were between 27 dB and 34 dB.

Samara and Ghadah [32] made a new lossy color compression of the YCbCr base by combining adaptive lossy 1-D polynomial coding, the MMSA of C421, and the Double Scalar Uniform Quantization System (DSUQS). The compression ratio is between 21 and 27, and the PSNR is between 36 and 38.

Ghadah et al. [33] introduced a novel lossy adaptive technique that exploits polynomial bases separately for each color band, where coefficients are compressed losslessly while residuals (prediction error) are compressed lossily with minimal loss to ensure higher performance in terms of compression ratios (gain), which are between 3 and 6, and pleasant reconstructed quality, where PSNR values are between 32 dB and 52 dB on average.

### 3. The proposed system

In this paper, the polynomial coding of the modeling base is utilized to compress grayscale lossily with DWT decomposition and quantization schemes, and the encoding process is composed of the steps discussed below. Also, Fig. 1 shows the proposed compression system clearly.

**Step 1:** Use uncompressed input grayscale square  $I$  (i.e., size  $N \times N$ ) of BMP format.

**Step 2:** Apply multi-scheme decomposition of three layers of Haar DWT, where  $I$  decomposed into approximation sub-bands and details sub-bands hierarchically, of sizes  $(N/2 \times N/2)$ ,  $(N/4 \times N/4)$  and  $(N/8 \times N/8)$ , respectively.

**Step 3:** Perform the 2D linear polynomial coding technique for the approximation sub-band ( $LL_3$ ) that consists of the following sub-steps [27]:

1- Partition the ( $LL_3$ ) into non-overlapped blocks of fixed size  $n \times n$  ( $4 \times 4$ ).

2- Find the estimated linear polynomial coefficients using Eq. (1-3).

$$a_0 = \frac{1}{n \times n} \sum_{i=0}^{n-1} \sum_{j=0}^{n-1} I(i, j) \quad (1)$$

$$a_1 = \frac{\sum_{i=0}^{n-1} \sum_{j=0}^{n-1} I(i, j) \times (j - x_c)}{\sum_{i=0}^{n-1} \sum_{j=0}^{n-1} (j - x_c)^2} \quad (2)$$

$$a_2 = \frac{\sum_{i=0}^{n-1} \sum_{j=0}^{n-1} I(i, j) \times (i - y_c)}{\sum_{i=0}^{n-1} \sum_{j=0}^{n-1} (i - y_c)^2} \quad (3)$$

where the computed coefficients are represented by  $a_0$ , which corresponds to the fixed block mean, while  $a_1$  and  $a_2$  correspond to the ratio of intensity block pixels from the block center ( $x_c$ ,  $y_c$ ) to the squared distance in  $i$  and  $j$  coordinates [20].

$$xc = yc = \frac{n-1}{2} \tag{4}$$

3- Quantize/dequantize the computed coefficients uniformly, where each coefficient is quantized using a different quantization step [26].

$$a_0Q = \text{round} \left( \frac{a_0}{QS_{a0}} \right) \rightarrow a_0D = a_0Q \times QS_{a0} \tag{5}$$

$$a_1Q = \text{round} \left( \frac{a_1}{QS_{a1}} \right) \rightarrow a_1D = a_1Q \times QS_{a1} \tag{6}$$

$$a_2Q = \text{round} \left( \frac{a_2}{QS_{a2}} \right) \rightarrow a_2D = a_2Q \times QS_{a2} \tag{7}$$

Where  $a_0Q, a_1Q, a_2Q$  are the uniform linear polynomial quantized values,  $QS_{a0}, QS_{a1}, QS_{a2}$  are the linear polynomial coefficients quantization steps and  $a_0D, a_1D, a_2D$  are dequantized linear polynomial values.

4- Encode the quantized coefficients using a probability base encoder.

5- The predicted image created using the linear polynomial coefficients dequantized values along the distance from the center for each segmented fixed block, such as [17]:

$$\tilde{I} = a_0D + a_1D(j - x_c) + a_2D(i - y_c) \tag{8}$$

6- The residual (prediction error) computed as a difference between the original and predicted approximation sub-bands (resultant from step above)  $\tilde{I}$  [8,27]

$$Res(i, j) = I(i, j) - \tilde{I}(i, j) \tag{9}$$

7- Encode the residual image (Res) using non-uniform quantization, which divides the range of the residue image into non-uniform slices with the same density for the positive and negative numbers and then determines the centroid of each slice of positive and negative numbers to represent all residue values for that slice. Algorithm (1) summarizes the non-uniform quantization steps. The residual is effectively quantized and dequantized using a quantization matrix of non-uniform bases [28].

$$ResQ = \text{round} \left( \frac{Res}{Q_{ResNon}} \right) \rightarrow ResD = ResQ \times Q_{ResNon} \tag{10}$$

where the non-uniform quantization matrix corresponds to  $Q_{ResNon}$ , and ResQ, ResD represent the quantized/dequantized residual images, respectively.

8- Encode and decode the quantized residual component using the arithmetic coding technique.

9- Rebuild the decoded image by adding the predicted (step 5) image and the dequantized residual image, as in Eq. (11) [28].

$$\hat{I}(i, j) = \tilde{I}(i, j) + ResD(i, j) \tag{11}$$

**Step 4:** Find the separation step using a hierarchical scheme for detail sub-bands (LH<sub>1</sub>, HL<sub>1</sub>, HH<sub>1</sub>, LH<sub>2</sub>, HL<sub>2</sub>, HH<sub>2</sub>, LH<sub>3</sub>, HL<sub>3</sub>, HH<sub>3</sub>) of the three levels using the following equation [32].

$$h = \begin{cases} SepStp_w \alpha^{w-1} & \text{for LH, HL in } w^{th} \text{ level} \\ SepStp_w \beta \alpha^{w-1} & \text{for HH in } w^{th} \text{ level} \end{cases} \tag{12}$$

where w is the wavelet level number and separation step ( $SepStp_w$ ),  $\alpha, \beta$  are separation parameters (such that,  $SepStp \geq 1, \alpha \leq 1, \beta \geq 1$ ) and h is the value of the cut point bit.

**Step 5:** Decompose the detail sub-bands into the most and least significant values (MSV and LSV) and compute the values for each of the three levels of detail sub-bands [33].

$$I_{MSV} = \text{round} \left( \frac{I}{Separation} \right) \tag{13}$$

$$I_{LSV} = I - (I_{MSV} \times Separation) \tag{14}$$

where I refers to the original image, and separation is the cutting point bit values, which control the parameter that isolated the image value range, as well as  $IMS$ V and  $ILSV$ , which correspond to the most and least significant values, respectively.

**Step 6:** Use iterative scalar uniform quantization to compress the most significant image value (MSV) that is composed of the following steps:

1. Converting each of the most significant values (MSV) from a 2D array into a 1D array
2. Perform the quantization of the iterative basis to find the iteration and the remainder of each value by determining the accuracy [34].

$$Positions = integer(positions \times 10) \tag{15}$$

3. Encoding the soft thresholding results using the Lempel-Ziv coding method and Huffman coding

**Step 7:** Apply a soft quantization thresholding scheme to compress the least significant value (LSV) that is composed of the following steps:

1. Identifying the differences between the level three and level one detailed sub-bands and rounding the difference results according to Eq. (16–18).

$$Th_{LH} = round(LH_3 - LH_1) \tag{16}$$

$$Th_{HL} = round(HL_3 - HL_1) \tag{17}$$

$$Th_{HH} = round(HH_3 - HH_1) \tag{18}$$

2. Applying the soft quantization thresholding scheme to the detailed sub-bands of each level separately, using the factor of each one of the detailed sub-bands as the threshold that can be different at each time in the following soft thresholding equations

$$I_{LH}Q = \begin{cases} Sign(I_{LH}) & \text{if } |I_{LH}| \geq Th_{LH} \\ 0 & \text{else} \end{cases} \tag{19}$$

$$I_{HL}Q = \begin{cases} Sign(I_{HL}) & \text{if } |I_{HL}| \geq Th_{HL} \\ 0 & \text{else} \end{cases} \tag{20}$$

$$I_{HH}Q = \begin{cases} Sign(I_{HH}) & \text{if } |I_{HH}| \geq Th_{HH} \\ 0 & \text{else} \end{cases} \tag{21}$$

3. Encoding the soft thresholding results using the Lempel-Ziv coding [35] method and Huffman coding [36]

**Step 8:** Perform the following steps to explain the **decoding process**: For the decoding polynomial, add the estimated image to the dequantized residual one using Eq. (22) to reconstruct the decoded image  $\hat{I}(i, j)$ . Also, Fig. 2 shows the proposed decompression system clearly.

$$\hat{I}(i, j) = \tilde{I}(i, j) + ResD(i, j) \tag{22}$$

**Step 9:** Apply the inverse of the most significant value to obtain the decoded MSV of each detail subband of the three levels according to Eq. (23–25).

$$Positions = \frac{Positions}{10} \tag{23}$$

$$Values = 2^{Number\ of\ Divisions} \tag{24}$$

$$\hat{I} = round(Values \times Position) \tag{25}$$

**Step 10:** Return the decoded MSV from 1-D into 2-D array

**Step 11:** Multiply the decoded MSV by the separation value to obtain the reconstructed MSV of each detail subband of the three levels.

$$RI_{MSV} = \hat{I}_{MSV} \times Separation \tag{26}$$

Where  $RI_{MSV}$  corresponds to the reconstructed MSV detail subbands,  $\hat{I}_{MSV}$  is the decoded MSV of detail subbands, and  $Separation$  is the value of the cut point bit.

**Step 12:** Add the reconstructed MSV of each detail subband of the three levels to the decoded LSV to obtain the reconstructed detail subbands.

$$RI_{details} = RI_{MSV} + RI_{LSV} \tag{27}$$

where  $RI_{MSV}$ ,  $RI_{LSV}$  correspond to the reconstructed MSV and LSV of detail subbands, and  $RI_{details}$  are the reconstructed detail subbands.

**Step 13:** Apply the inverse of the DWT of the hierarchal scheme of each band to reconstruct the decoded image.

**Step 14:** Reconstruct the approximated compressed by adding the inverse of the polynomial technique and the inverse of the most and least significant values to the inverse of the DWT.

**Algorithm 1:** Non-uniform residual quantization process

Input: Sample(0..ImageSize-1) which corresponds to residual image (Res)  
Q as the attained Quantization Range

**Step 1:** Define the Lowest and Highest Value

```
Max=Sample(i): Min=Sample(i)
for i=0 to ImageSize-1: S=Sample(i)
  if Min>S then Min=S else if Max<S then Max=S
next i
```

**Step 2:** Determine the Histogram for the positive and Negative Values

```
redim HistN(Min), HisP(Max)
NonZN=0: NonZP=0
for I=0 to ImageSize-1: S=Sample(i)
  if S<0 then
    S=-S: HistN(S)=HistN(S)+1: NonZN=NonZN+1
  else
    HistP(S)=HistP(S)+1: NonZP=NonZP+1
next I
NonZ=NonZN+NonZP
```

**Step 3:** Determine the Accumulated Histogram

```
redim AcnN() as byte, AcnP() as byte
NonZR=0.5*(Wid×Hgt-NonZ)/(Wid×Hgt)
AcmN(0)=NonZR: AcnP(0)=NonZR
for i=1 to Min: AcnN(i)=AcnN(i-1)+HisN(i)/NonZN: next i
for i=1 to Max: AcnP(i)=AcnP(i-1)+HisP(i)/NonZP: next i
```

**Step 4:** Build the lookup table

```
Rng=Q/2
for i=1 to Min: TblN(i)=AcnN(i) ×Rng: next i
for i=1 to Max: TblP(i)=AcnP(i) ×Rng: next i
for i=0 to ImageSize-1: S=Sample
  if S=0 then qSamp(i)=0
  elseif S>0 then qSamp(i)=TblP(S)
  elseif S<0 then qSamp(i)=-TblN(S)
next i
```

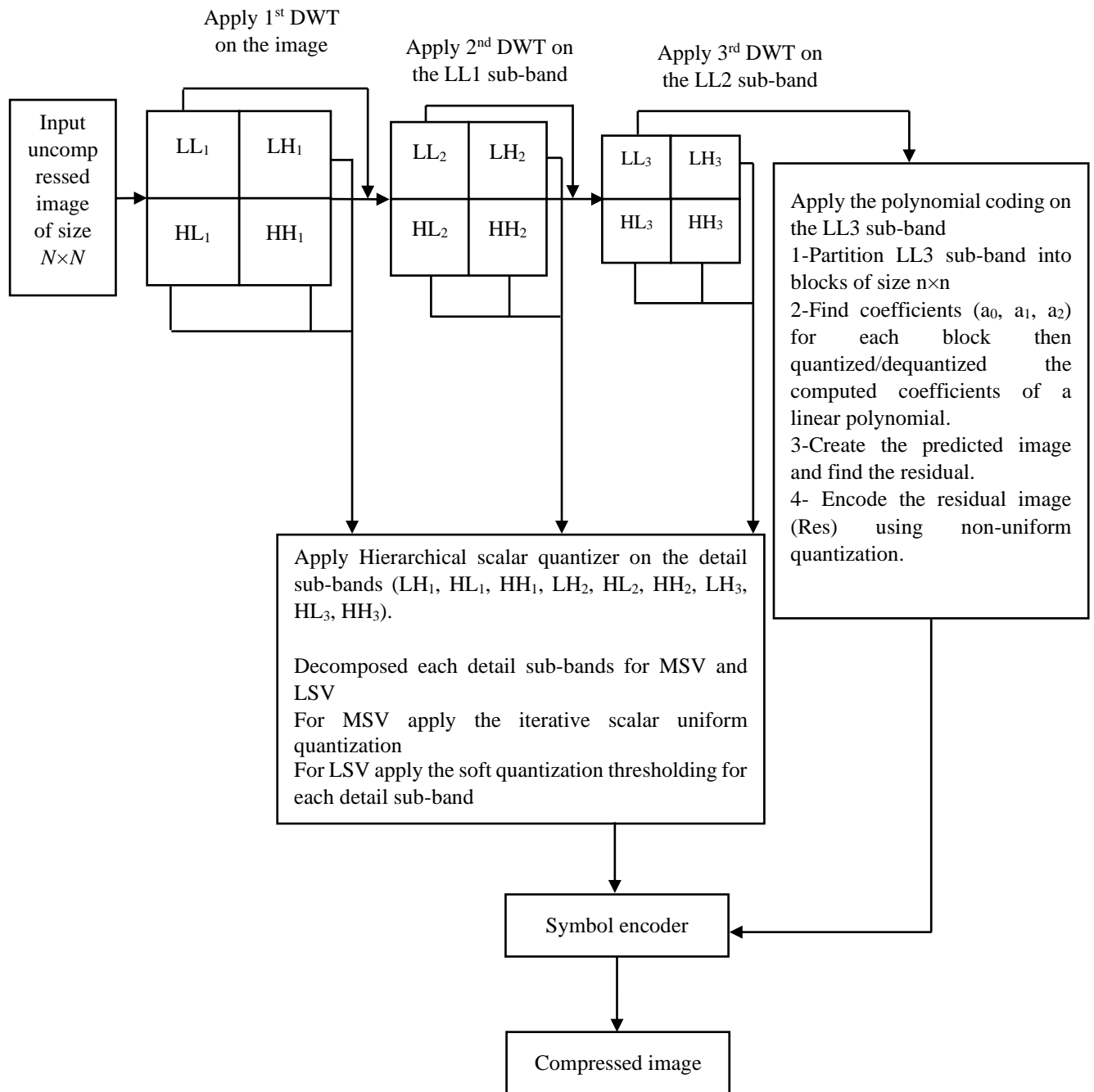


**Figure 1:** Structure and encoding of the proposed system

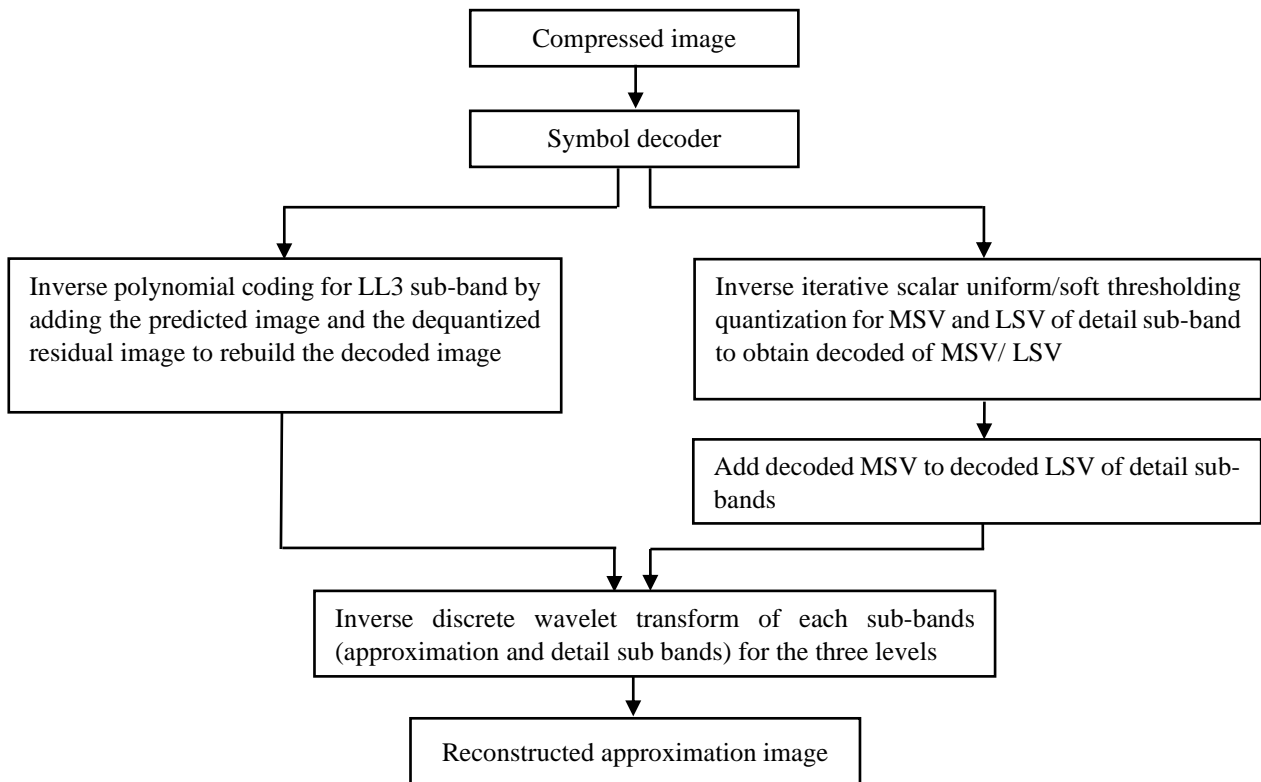


**Figure 2:** Structure and decoding of the proposed system

**4. Results and Discussion**

For testing the suggested compression system performance, five standard square images of size 256×256 were adopted, as shown in Fig. 3.

The compression ratio measure corresponds to the ratio of the original image size in bytes to the compressed size of image information in bytes, along with an objective fidelity measure of the peak signal-to-noise ratio (PSNR) between the original image  $I$  and the decoded image  $\hat{I}$ .

$$PSNR(I, \hat{I}) = 10 \log_{10} \left( \frac{(\text{maximum gray scale of image})^2}{MSE} \right) \tag{28}$$

$$MSE(I, \hat{I}) = \frac{1}{n \times n} \sum_{i=0}^{n-1} \sum_{j=0}^{n-1} [\hat{I}(i, j) - I(i, j)]^2 \tag{29}$$

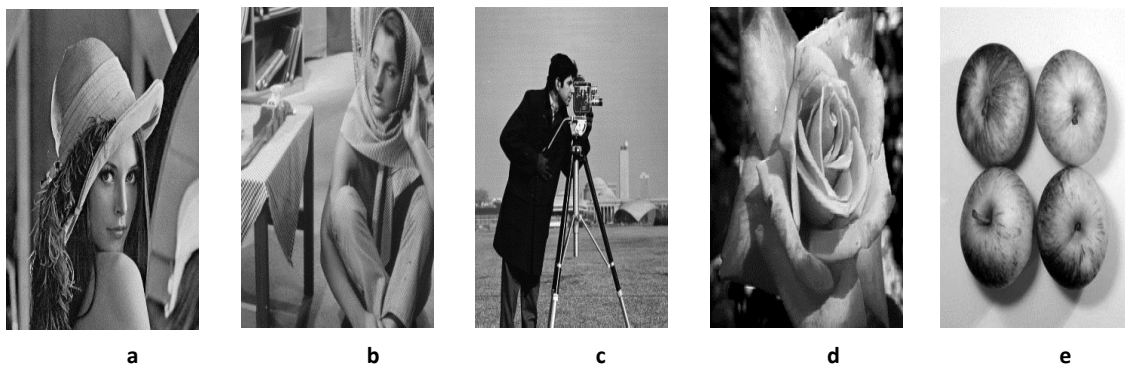


**Figure 3:** The adopted images are (a) Lena image, (b) Barbara image, (c) Cameraman image, (d) Rose image, and (e) Apple image, all images of size 256×256 images.

Table 1 shows the considered dominant parameters, whose values have been tested in detail. The results are shown in Table 2 and Table 3, which summarize the compression ratio, PSNR, and separation parameters used for the five tested images.








It is clear that the increase in values for the detail subbands of the three levels of DWT affected the performance of the proposed technique in terms of compression ratio and *PSNR*, where small values mean a small compression ratio and a high *PSNR*, and vice versa. For the approximation sub-band of the third level, the polynomial coding consists of two parts: the first part is the coefficients ( $a_0, a_1, a_2$ ), which are quantized uniformly, with  $a_0$  equal to 16 and  $a_1$  and  $a_2$  equal to 32, and the second part is the residual part, which is quantized non-uniformly and equal to 32.

Table 2 shows the system performance increases and decreases in *PSNR* values when the control parameters ( $\alpha, \beta$ ) are increased. Increasing the number of digits improves the compression ratio, as demonstrated in Table 3.



**Table 1:** The selected values of the control parameters

Proposed compression system			
Parameter value	Range value	Parameter value	Range value
nxn	4×4	Alpha $\alpha$	[0.7, 0.8, .....2.4]
Qa <sub>0</sub>	16	Beta $\beta$	[0.8, 1.0, .....4.2]
Qa <sub>1</sub> , Qa <sub>2</sub>	32	Number of digits	10, 100
QRes	32	Accuracy Range	[5 2]
Separation	5		

**Table 2:** The tested results of the proposed technique

Tested Image	Separation =5 No. of Digits=10 Accuracy Range = [5 2]				
	Alpha	Beta	CR	PSNR	Encode/Decode Time (sec)
 Lena	0.7	0.8	10.0763	38.6238	8.0781
	1.5	2.4	13.4792	37.1573	7.9219
	1.9	3.2	15.4639	34.6709	7.2656
	2.2	3.8	16.0235	32.5070	6.7188
	2.4	4.2	16.2459	30.7510	6.5000
 Barbara	0.7	0.8	9.9963	39.7154	7.6094
	1.5	2.4	13.4460	37.9192	7.5156
	1.9	3.2	15.4348	34.4805	6.5469
	2.2	3.8	16.1022	32.1125	6.3594
	2.4	4.2	16.3758	31.4287	6.2969
 Cameraman	0.7	0.8	10.7190	41.1678	7.1719
	1.5	2.4	14.6286	39.4013	6.6250
	1.9	3.2	16.8733	36.4074	6.2188
	2.2	3.8	17.3928	33.7463	6.2031
	2.4	4.2	17.6267	32.0676	6.0625
 Rose	0.7	0.8	10.9427	39.8490	6.8594
	1.5	2.4	14.6909	37.8867	6.6563
	1.9	3.2	17.1246	34.8254	6.4688
	2.2	3.8	17.7942	32.8346	6.3906
	2.4	4.2	18.1089	32.1257	6.1094
 Apple	0.7	0.8	11.5421	40.6373	6.4063
	1.5	2.4	16.2298	38.7224	6.2188
	1.9	3.2	18.7998	36.2204	5.8750
	2.2	3.8	19.4353	34.4396	5.8594
	2.4	4.2	19.6451	33.3862	5.6719

**Table 3:** The tested results of the proposed technique

Tested Image	Separation =5 No. of Digits=100 Accuracy Range = [5 2]				
	Alpha	Beta	CR	PSNR	Time
Lena 	0.7	0.8	13.3911	38.6983	5.7969
	1.0	1.4	13.4626	38.4432	5.5469
	1.5	2.4	17.1470	37.2050	5.4844
	1.9	3.2	19.7279	34.6964	5.0938
Rose 	0.7	0.8	14.4767	39.9319	5.6406
	1.0	1.4	14.5733	39.6423	5.4688
	1.5	2.4	18.6023	37.9351	5.2188
	1.9	3.2	21.6505	34.8483	5.1250

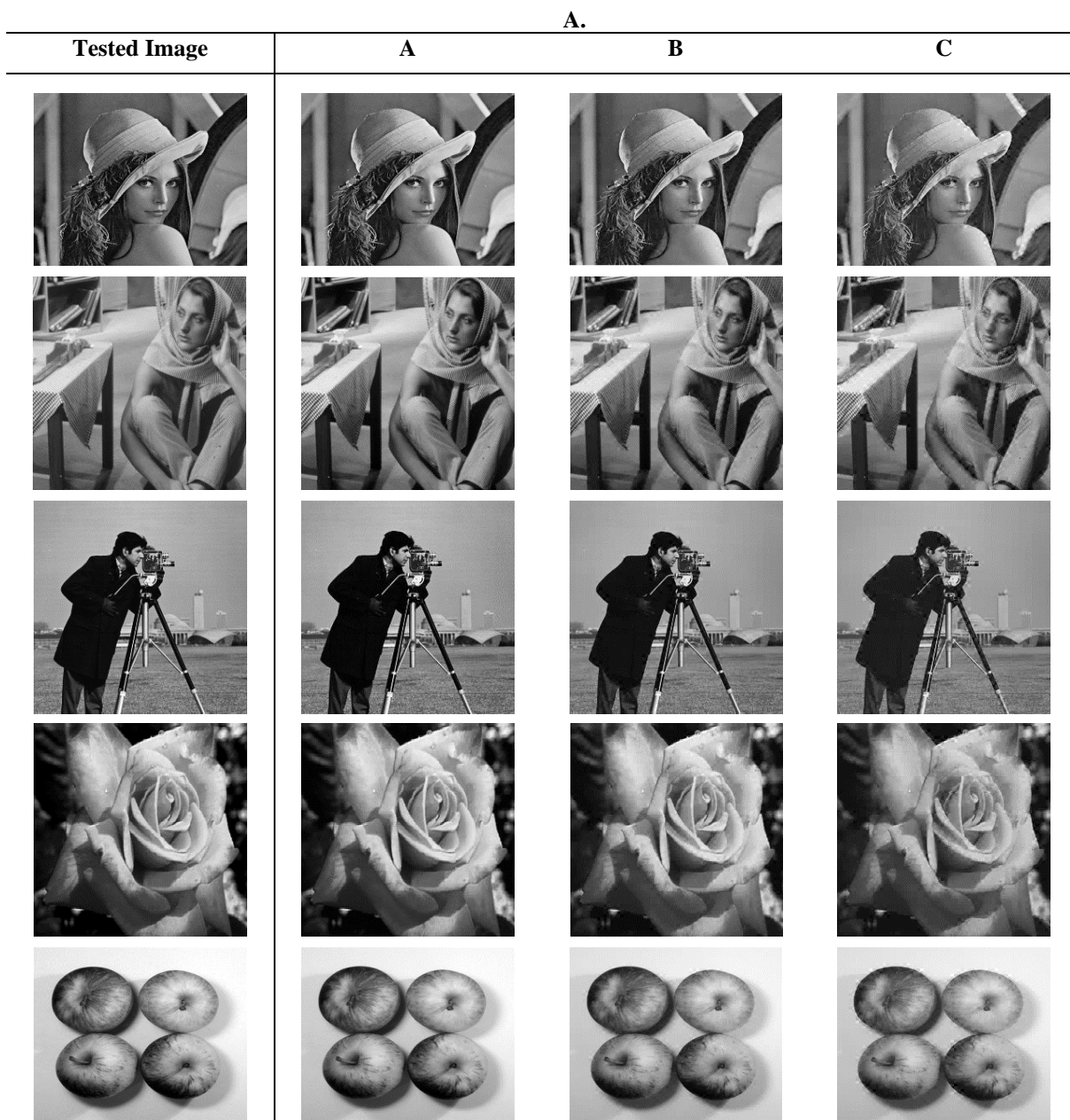


**Figure 4:** The compressed images using the proposed system techniques Making Separation = 5 and No. of Digits = 10 **A-** alpha = 0.7 and beta = 0.8. **B-** alpha = 1.9 and beta = 3.2. **C-** alpha = 2.4 and beta = 4.2

### 5. Comparative Evaluation

In this work, a comparative evaluation was performed in Table 4 to demonstrate the robustness of the suggested method, where the comparison indicates the CR and PSNR measures for five images with block size 4×4, separation equal to 5, number of digits equal to 10, and accuracy range [5 2] with values of  $\alpha = 0.7$  and  $\beta = 0.8$ . From Table 4, the outcomes show that the suggested techniques have a higher compression ratio than JPEG while decreasing the image quality, as shown in Fig. 5. In Table 5, [28] used three images of block size 4×4, where the CR is between [2.3788–2.5149], while the CR for the suggested system is between [10.0763–10.9427], as shown in Fig. 6.

**Table 4:** Compression of the Standard JPEG with the Proposed Compression System

Tested Image	JPEG		Proposed system	
	CR	PSNR (dB)	CR	PSNR (dB)
Lena	7.5919	33.6085	10.0763	38.6238
Barbara	7.4332	33.8662	9.9963	39.7154
Cameraman	8.7912	34.2935	10.7190	41.1678
Rose	7.9404	35.8628	10.9427	39.8490
Apple	10.0787	37.0543	11.5421	40.6373

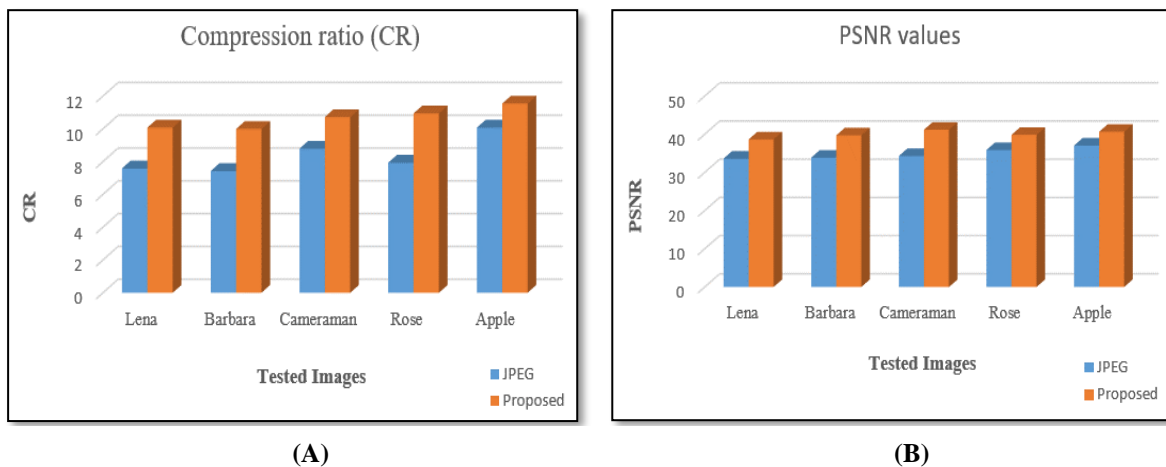


**Figure 5:** Comparison performance between the standard JPEG and the proposed system in terms of (a) CR and (b) PSNR

**Table 5:** Compression of the Proposed Compression System with Article [28] in terms of CR and PSNR

Tested Image	Article [28]		Proposed system		JPEG	
	CR	PSNR (dB)	CR	PSNR (dB)	CR	PSNR (dB)
Lena	2.3788	51.4905	10.0763	38.6238	7.5919	33.6085
Cameraman	2.5149	55.2948	10.7190	41.1678	7.9404	35.8628
Rose	2.3344	50.4196	10.9427	39.8490	8.7912	34.2935

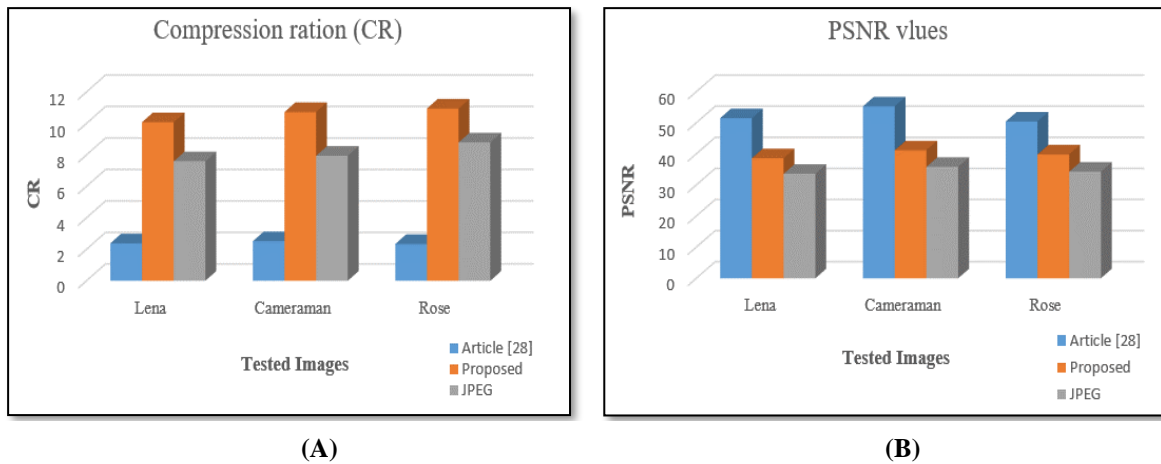


**Figure 6:** Comparison performance between the standard JPEG, the proposed system, and article [28] in terms of (a) CR and (b) PSNR

## 6. Conclusion

This paper investigates an effective hybrid lossy technique for compressing grayscale natural images, with the main conclusions being:

- The proposed system used polynomials as a spatial technique along with DWT decomposition.
- The mixing of quantization techniques efficiently improves results in terms of compression ratio and PSNR.
- The proposed system uses uniform scalar quantization for coefficients and non-uniform scalar quantization for residual images to maintain image quality without degradation.
- The use of hierarchal separation with various control parameters increases the compression ratio and decreases the PSNR value when the control parameter is increased.
- The use of an iterative scalar quantizer for MSV with different numbers of digits improved compression performance.

## References

- [1] A. A. Hussain, G. K. AL-Khafaji and M. M. Siddeq, "Developed JPEG Algorithm Applied in Image Compression," *2nd International Scientific Conference of Al-Ayen University, Materials Science and Engineering Conference Series*, vol. 928, pp. 1-17, 2020, doi:10.1088/1757-899X/928/3/032006.
- [2] M. H. Rasheed, O. M. Salih and M. M. Siddeq, "Joint image encryption and compression schemes based on hexa-coding," *Periodicals of Engineering and Natural Sciences (PEN)*, vol. 9, no. 2, pp. 569-580, 2021, doi:pen.ius.edu.ba/index.php/pen/article/view/1839/794.
- [3] Z. H. Abed and G. Al-Khafaji, "Pixel Based Techniques for Gray Image Compression: A review," *Journal of Al-Qadisiyah for Computer Science and Mathematics*, vol. 14, no. 2, pp. 59–70, 2022, doi.org/10.29304/jqcm.2022.14.2.967.
- [4] Y. A. Salih, A. A. Mohammed and L. E. George, "Improved Image Compression Scheme Using Hybrid Encoding Algorithm," *Kurdistan Journal of Applied Research (KJAR)*, vol. 4, no. 2, pp. 90-101, 2019, Doi: 10.24017/science.2019.2.9.
- [5] N. H. Salman and S. Rafea, "The Arithmetic Coding and Hybrid Discrete Wavelet and Cosine Transform Approaches in Image Compression," *Journal of Southwest Jiaotong University*, vol. 55, no. 1, pp. 1-9, 2020, Doi: 10.35741/issn.0258-2724.55.1.6.
- [6] A. H. Ahmed and L. E. George, "The use of wavelet, DCT & quadtree for color image compression," *Iraqi Journal of Science*, vol. 58, no. 1C, pp. 550-561, 2017.

- [7] A. S. Abd-Alzhra and M. S. H. Al- Tamimi, "Image Compression Using Deep Learning: Methods and Techniques," *Iraqi Journal of Science*, vol. 63, no. 3, pp. 1299-1312, 2022, Doi: 10.24996/ij.s.2022.63.3.34.
- [8] G. Al-Khafaji and H. B. Al-Kazaz, "Adaptive Color Image Compression of Hybrid Coding and Inter- Differentiation Based Techniques," *International Journal of Computer Science and Mobile Computing*, vol. 8 no.11, pp. 65-70, 2019.
- [9] A. A. Hussain, "Photo Passport Compression using Hybrid Techniques," M.S. thesis, Dept. of Comp. Sci., Coll. of Sci., Univ. Baghdad, Al-Jadriya, Baghdad, Iraq, 2021.
- [10] R. I. Yousif and N. H. Salman, "Image Compression Based on Arithmetic Coding Algorithm," *Iraqi Journal of Science*, vol. 62, no. 1, pp. 329-334, 2021, Doi: 10.24996/ij.s.2021.62.1.31.
- [11] S. G. Mohammed, S. S. Abdul-Jabbar and F. G. Mohammed, "Art Image Compression Based on Lossless LZW Hashing Ciphering Algorithm," In *Journal of Physics: Conference Series, 3rd International Conference in Physical Science and Advanced Materials (PAM 2021)*, Istanbul, Turkey, 2021, doi:10.1088/1742-6596/2114/1/012080.
- [12] Z. J. Ahmed and L. E. George, "A Comparative Study Using LZW with Wavelet or DCT for Compressing Color Images," *International Conference on Advanced Science and Engineering (ICOASE), IEEE*, Iraq, pp. 53-58, 2020, Doi: 10.1109/ICOASE51841.2020.9436622.
- [13] Z. J. Ahmed, L. E. George and R. A. Hadi, "Images Compression using Combined Scheme of Transform Coding," *Journal of Engineering Research and Sciences*, vol. 1, no. 9, pp. 8-14, 2022, Doi: dx.doi.org/10.55708/js0109002.
- [14] O. K. Obayes "Polynomial Color Image Compression using Joint and Different Models," High Diploma Dissertation, Dept. of Comp. Sci., Coll. of Sci., Univ. Baghdad, Al-Jadriya, Baghdad, Iraq, 2020.
- [15] N. Ahmad, Z. A. Jaffery and Irshad, "An Approach to Color Image Coding Based on Adaptive Multilevel Block Truncation Coding," *In Applications of Artificial Intelligence Techniques in Engineering*, vol. 2, pp. 597-606, Springer Singapore, 2019, Doi: org/10.1007/978-981-13-1822-1\_56.
- [16] X. Liu, P. An, Y. Chen, and X. Huang, "An Improved Lossless Image Compression Algorithm based on Huffman Coding," *Multimedia Tools and Applications*, vol. 81, no. 4, pp. 4781–4795, 2022, Doi: org/10.1007/s11042-021-11017-5.
- [17] G. Al-Khafaji, A. A. Hussain, and U. S. Al-Hasani, "Hierarchal Polynomial Coding of Grayscale Lossless Image Compression," *International Journal of Computer Science and Mobile Computing*, vol 8, no 6, pp. 165-171, 2019.
- [18] N. S. Mahdi, "Image Compression based on Adaptive Polynomial Coding," High Diploma Dissertation, Dept. of Comp. Sci., Coll. of Sci., Univ. Baghdad, Al-Jadriya, Baghdad, Iraq, 2015.
- [19] Z. J. Ahmed, L. E. George, "Lightweight Image Compression Using Polynomial and Transform Coding," *V. International Scientific Congress of Pure, Applied and Technological Sciences (Minar Congress)*, Rimar Academy Turkey, pp.172-192, 2022.
- [20] N. S. Mahdi and G. Al-Khafaji, "Image Compression using Polynomial Coding Techniques: A review," *Journal of Al-Qadisiyah for Computer Science and Mathematics*, vol. 14, no. 2, pp. 70–81, 2022, doi:10.29304/jqcm.2022.14.2.968 1.
- [21] G. Al-Khafaji, and M. Bassim, "Polynomial Color Image Compression," *International Journal of Engineering Trends and Technology (IJETT)*, vol. 61, no. 3, pp. 161-165, 2018. Available: <https://ijettjournal.org/assets/year/2018/volume-61/IJETT-V61P226.pdf>
- [22] R. T. Al-Tamimi, "Intra Frame Compression using Adaptive Polynomial Coding," M.S. thesis, Dept. of Comp. Sci., Coll. of Sci., Univ. Baghdad, Al-Jadriya, Baghdad, Iraq, 2015.
- [23] A. T. khudhair, "Adaptive Polynomial Coding for Image Compression," High Diploma Dissertation, Dept. of Comp. Sci., Coll. of Sci., Univ. Baghdad, Al-Jadriya, Baghdad, Iraq, 2015.
- [24] S. D. Ahmed, "Adaptive Polynomial Transform Coding," M.S. thesis, Dept. of Comp. Sci., Coll. of Sci., Univ. Baghdad, Al-Jadriya, Baghdad, Iraq, 2016.

- [25] R. T. Al-Timimi, "Bit Plane Slicing, Wavelet and Polynomials Mixing for Image Compression," *Iraqi Journal of Science*, vol. 60, no. 11, pp. 2497-2505, 2019, Doi: 10.24996/ijs.2019.60.11.22
- [26] G. Al-Khafaji, N. S. Mahdi, and U. S. Al-Hasani, "Hybrid Color Image Compression of Hard & Soft Mixed Thresholding Techniques," *International Journal of Computer Science and Mobile Computing*, vol 5, no 7, pp. 375-381, 2016.  
Available: <https://ijcsmc.com/docs/papers/July2016/V5I7201647.pdf>.
- [27] G. Al-Khafaji, "Linear Polynomial Coding with Midtread Adaptive Quantizer," *Iraqi Journal of Science*, vol. 59, no.1c, pp. 585-590, 2018, Doi: 10.24996/IJS.2018.59.1C.15.
- [28] G. Al-Khafaji and L. E. George, "Grey-Level Image Compression Using 1-D Polynomial and Hybrid Encoding Techniques," *Journal of Engineering Science and Technology*, vol. 16, no. 6, pp. 4707-4728, 2021.  
Available:[https://jestec.taylors.edu.my/Vol%2016%20Issue%206%20December%202021/16\\_6\\_25.pdf](https://jestec.taylors.edu.my/Vol%2016%20Issue%206%20December%202021/16_6_25.pdf).
- [29] S. S. AL-Hadithy, G. Al-Khafaji and M. M. Siddeq, "Adaptive 1-D Polynomial Coding of C621 Base for Image Compression," *Turkish Journal of Computer and Mathematics Education*, vol. 12, no. 13, pp. 5720-5731, 2021.  
Available: <https://www.turcomat.org/index.php/turkbilmate/article/view/9823/7507>
- [30] R. T. Gdeeb, G. Al-Khafaji and N. Ali, "Development of Hybrid Based Lossless Iris Image Compression Technique," *International Journal of Engineering Research and Advanced Technology (IJERAT)*, vol. 8, no.7, pp. 11-16, 2022, Doi: 10.31695/IJERAT.2022.8.7.2.
- [31] Z. J. Ahmed, L. E. George and R. A. Hadi, "Image Signal Decomposition Using Polynomial Representation with Hybrid Lossy and Non-Lossy Coding Scheme," *Iraqi Journal of Science*, vol. 63, no. 10, pp. 4559-4575, 2022, Doi: 10.24996/ijs.2022.63.10.38.
- [32] S. S. AL-Hadithy and G. Al-Khafaji, "Adaptive 1-D polynomial coding to compress color image with C421," *International Journal of Nonlinear Analysis and Applications*, vol. 14, no. 1, pp. 1261-1276, 2023, Doi: 10.22075/ijnaa.2023.7013.
- [33] G. Al-Khafaji, M. H. Rasheed, M. M. Siddeq and M. A. Rodrigues, "Adaptive Polynomial Coding of Multi-Base Hybrid Compression," *International Journal of Engineering, Transactions B: Applications*, vol. 36, no. 2, pp. 236-252, 2023, Doi: 10.5829/ije.2023.36.02b.05.
- [34] B. A. Sultan and L. E. George, "Color image compression based on spatial and magnitude signal decomposition," *International Journal of Electrical and Computer Engineering (IJECE)*, vol. 11, no.5, pp. 4069-4081, 2021, Doi: 10.11591/ijece.v11i5.pp4069-4081.
- [35] A. Y. Maghari, "A Comparative Study of DCT and DWT Image Compression Techniques Combined with Huffman Coding," *Jordanian Journal of Computers and Information Technology (JJCIT)*, vol. 5, no. 2, pp. 73-86, 2019, Doi: 10.5455/jjcit.71-1554982934
- [36] H. Kaur, S. Mahey and N. Kuar, "Image Compression Techniques with LZW method," *International Journal for Research in Applied Science and Engineering Technology (IJRASET)*, vol. 10, no. 1, pp. 1773-1777, 2022, Doi: 10.22214/ijraset.2022.39999.